

## Chapter 2

# Needle Insertion in Simulated Soft Tissue

**Abstract** This chapter presents the very first application of the cutaneous-only sensory subtraction approach in teleoperation. It considers a simulated needle insertion in soft tissue along one direction. Part of the needle workspace is protected by a forbidden-region stiff active constraint, which is a common scenario for biopsies, deep brain stimulation and functional neurosurgery. Subjects are required to insert the needle inside the simulated soft tissue and stop the motion of the tool as soon as the presence of the stiff constraint is felt. The motion of the needle is controlled through an Omega 3 haptic interface. Accordingly to the sensory subtraction approach, the haptic feedback provided by the Omega 3 is substituted with cutaneous feedback provided by a pair of ungrounded fingertip cutaneous devices. Experiments show that the proposed cutaneous-only feedback approach, other than being intrinsically stable, improves teleoperation performance with respect to other sensory substitution techniques, such as the one using visual feedback in substitution of haptic feedback.

## 2.1 Introduction

Force feedback is helpful during needle advancement to detect local mechanical properties of the tissue and to distinguish between expected and abnormal resistance due, for example, to the unexpected presence of vessels or to the action of active constraints. Active constraints are software functions used in assistive robotic systems to regulate the motion of surgical tools. The motion of the surgical tool, the needle in our case, is still controlled by the surgeon, but the system constantly monitors its motion and takes some actions if it fails to follow a predetermined procedure. Active constraints play two main roles: they can either guide the motion of the tool or strictly forbid the surgeon from reaching certain regions [1]. A guiding active

---

This chapter is reprinted with kind permission from IEEE, originally published in [2].

constraint attenuates the motion of the surgical tool in some predefined directions to encourage the surgeon to conform to the procedure plan. A forbidden-region active constraint seeks to prevent the needle from entering a specific region of the workspace. Forbidden-region active constraints may be introduced to protect areas that must be avoided to prevent damage of tissue and of its functionality. This is the case, for instance, of brain surgery, in which tissue manipulation in certain areas can cause serious injury to patients.

In this work we consider a simulated needle insertion in soft tissue along one direction. Part of the needle workspace is protected by a forbidden-region stiff active constraint. This is a common scenario for biopsies, deep brain stimulation and functional neurosurgery [3, 4]. Subjects are required to insert the needle inside the simulated soft tissue and stop the motion of the tool as soon as the presence of the stiff constraint is felt. The motion of the needle is controlled through an Omega 3 haptic interface. We propose to substitute the haptic feedback provided by the Omega 3 with cutaneous feedback provided by a pair of ungrounded fingertip cutaneous devices.

Section 2.2 gives a brief description of the cutaneous device used for the experiment. Sections 2.3 and 2.4 present and discuss the experimental evaluation, respectively. Finally, Sect. 2.5 addresses concluding remarks and perspectives of the work, together with its relevance for the other applications presented in the book.

## 2.2 An Ungrounded Fingertip Cutaneous Device

The 3-DoF ungrounded cutaneous device used in these experiments is shown in Fig. 2.1a. It consists of two platforms: one is located on the back of the finger, supporting three small DC motors, and the other one is in contact with the volar surface of the fingertip. The motors shorten and lengthen three cables to move the platform toward the user's fingertip and re-angle it to simulate contacts with arbitrarily oriented surfaces. The direction and amount of the force reflected to the user is changed

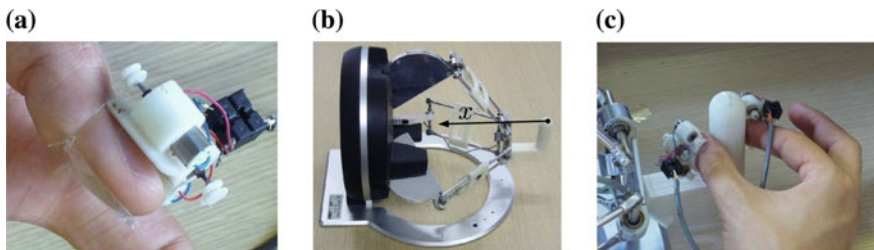


**Fig. 2.1** Experimental setup. Subjects were asked to wear two cutaneous devices on the *right hand* and grasp the Omega 3 handle as shown in Fig. 2.1c. Subjects were also asked to wear two additional cutaneous devices on the thumb and index finger of the *left hand*. The motion of the Omega 3 haptic device was limited along its  $x$ -axis by three clamps. **a** The cutaneous device. **b** Omega 3 grounded device. **c** The custom handle used by a subject during the insertion

by properly controlling the cable lengths. This device is an improved version of the display presented by Minamizawa et al. [5]. In particular, the improvement consists of using three motors and a 3-DoF parallel manipulator architecture to render forces at the finger pad [6]. This device can be also seen as a simplified version of the device presented by Prattichizzo et al. [7]. However, when we ran the experiments reported in this chapter, the ungrounded device of [7] was still in a very early stage of development.

Although this device is capable of orienting and translating the mobile platform in three-dimensional space, in this work we used it as a 1-DoF system (all motors pulled the cables together), so that only forces in the sagittal plane of the finger were actuated, roughly normal to the longitudinal axis of the distal phalanx.

## 2.3 Experimental Evaluation

### 2.3.1 *Experimental Setup*

The experimental setup is shown in Fig. 2.1. It is composed of an Omega 3 haptic interface and four prototypes of the cutaneous device presented in Sect. 2.2. Three clamps are applied to the Omega interface to reduce its degrees of freedom from three to one (the  $x$  axis in Fig. 2.1b). A custom plastic handle is attached to the Omega's end-effector to allow the subject to use the device with two fingers (see Fig. 2.1c). The Omega 3 is used as a haptic device of the impedance type: the position of the needle, moved by the human subject, is measured, and a force signal is fed back to the user through the actuation system. The force signal accounts for either the remote contact interaction of a slave robot, in a classical teleoperation scenario, or of the virtual environment, as in our simulated scenario. Subjects were asked to wear two cutaneous devices on the right hand, on the thumb and index fingers, and to use the handle as shown in Fig. 2.1c. To investigate the role of feedback localization with respect to the hand involved in the task, subjects were also asked to wear two additional cutaneous devices on the thumb and index fingers of the contralateral hand.

The haptic handle teleoperates the needle in a virtual environment simulating the insertion in soft tissue with a stiff constraint. The needle moves along a single axis as shown in Fig. 2.2, where the needle, the tissue surface, and the stiff constraint are shown. The stiff constraint and the portion of the needle inside the tissue surface are not shown to the subject. The contact force between the needle and the tissue is calculated according to a visco-elastic model. The subject steering the needle feels a resistive force while penetrating the tissue, and an opposite force while trying to pull the needle out. In real scenarios, these forces are either measured from force sensors or estimated from other parameters. In this work a simple simulation of the soft tissue is used. The aim of this work is not the design an accurate tissue simulator based, for example, on FEM techniques [8], but to validate the proposed sensory subtraction approach.



**Fig. 2.2** The virtual environment is composed of the needle (white), driven by the operator, the deformable tissue (cyan), and the stiff constraint (red). The position of the needle  $x_n$  is linked to the position of the haptic device end-effector. The stiff constraint and the portion of the needle inside the tissue surface are not shown to the subject. **a** No needle-tissue contact. **b** Needle reaches the tissue. **c** Needle penetrates the tissue (color figure online)

A spring  $k_t = 2 \text{ N/m}$  and a damper  $b_t = 5 \text{ Ns/m}$  are used to model the contact force  $f_t$  between the needle and the tissue, while a spring  $k_{sc} = 3000 \text{ N/m}$  is used to model the contact force  $f_{sc}$  between the needle and the stiff constraint. For the sake of simplicity, we assume that the mass of the tissue  $m_t = 1 \text{ kg}$  is concentrated at the contact point. The viscous coefficient of the body beneath the tissue is  $v_t = 0.7 \text{ Ns/m}$ .

As for the haptic rendering, the interaction is designed according to the god-object model [9] and the position of the Omega handle is linked to the needle position  $x_n$  moving in the virtual environment. The initial position of the surface of the tissue is set to  $\bar{x}_t = 20 \text{ mm}$  and the stiff constraint is located at  $\bar{x}_{sc}$ . Tissue position  $x_t$  changes according to the interaction with the needle, which is able to penetrate the surface only when the contact force  $f_h$  is larger than a predetermined threshold ( $f_p = 0.1 \text{ N}$ ). To extend the workspace in the virtual environment, we introduce a scale factor of 3 between the position of the needle and the subject's hand.

It is thus possible to discriminate four different operating conditions for the needle-environment interaction model here presented:

- no contact (see Fig. 2.2a),
- contact without penetration (see Fig. 2.2b),
- penetration within the safe area (see Fig. 2.2c), and
- penetration and contact with the stiff constraint.

In the first case, since the needle is out of the tissue, the model is designed to feed back no force to the subject and the surface of the tissue tends to return to its predetermined initial position  $\bar{x}_t$ . The dynamics of the interaction for the no contact case is therefore

$$\begin{cases} m_t \ddot{x}_t = -k_t (x_t - \bar{x}_t) - b_t \dot{x}_t, \\ f_h = 0. \end{cases}$$

When the needle touches the tissue, but the force  $f_h$  is not yet sufficient to penetrate it, the tissue surface is deformed by the movement of the needle. In this case, the dynamic model and the contact force to be fed back to the subject are

$$\begin{cases} x_t = x_n, \\ f_h = -k_t (x_t - \bar{x}_t) - b_t \dot{x}_t. \end{cases}$$

As soon as  $f_h > f_p$ , the needle penetrates the surface and while the needle is inside the tissue, the dynamics and the contact force are computed as

$$\begin{cases} m_t \ddot{x}_t = -k_t (x_t - \bar{x}_t) - b_t \dot{x}_t - v_t (\dot{x}_t - \dot{x}_n), \\ f_h = -v_t (\dot{x}_t - \dot{x}_n). \end{cases}$$

If the subject steers the needle toward the unsafe workspace area delimited by the stiff constraint, a force will be fed back to the subject in order to avoid the penetration of the needle in the forbidden area:

$$f_{sc} = -k_{sc} (x_n - \bar{x}_{sc}).$$

The haptic device measures the position of the subject's hand, sends it to the controller and then the virtual environment computes the force feedback and the dynamics of the tissue. The controller then sends the force back to the user through either the haptic device or the substitutive (cutaneous or visual) condition, as detailed in the next section.

### 2.3.2 Design of the Experiments

Four alternative feedback conditions were compared in the experiments: (full) *haptic* feedback, applied by the actuators of the haptic interface, *visual* feedback in substitution of haptic feedback, or *cutaneous* feedback in substitution of haptic feedback, applied by the ungrounded devices either on the fingers holding the handle or on the fingers of the contralateral hand. The substitutive visual feedback consisted in showing a horizontal bar depicting the contact force  $f_h$  registered at the needlepoint.

Subjects were asked to wear the four cutaneous devices for the whole duration of the experiments, and to grasp the handle with their right hand as shown in Fig. 2.1c. The subject's hand was positioned with its longitudinal axis at  $90^\circ$  from the Omega  $x$ -axis. The position of the subject's hand with respect to the joystick was checked before the beginning of each experiment. To prevent changes in the perceived direction of the feedback force generated by the Omega 3, subjects were instructed to move the forearm rather than the wrist while moving the device. During the experiments, the subjects maintained the initial orientation of the fingers with respect to the handle, which was the only natural way of grasping the handle for the 1-DoF task.<sup>1</sup>

---

<sup>1</sup>A modification of the way the fingers grasp the handle would imply that the perceived direction of the feedback force changes if haptic feedback is used, whereas it would not change with cutaneous-only feedback. This issue must be considered while trying to extend the sensory subtraction paradigm to multi-DoF tasks, since the results may be affected by this change of direction of the force vector. Thus, the position of the subject's hand with respect to the input device must be carefully monitored before and during the experiments.

The task consisted in inserting the needle into the soft tissue and stopping its motion as soon as the presence of the stiff constraint was perceived. After 5 s of continuous contact with the constraint, the system played a sound beep. Subjects were instructed to pull the needle out of the tissue as soon as the sound was heard. In all the considered conditions, regardless of particular feedback condition employed, visual feedback on needle insertion was provided to the subjects, showing the portion of the needle outside the tissue and the surface of the tissue. The stiff constraint and the portion of the needle inside the tissue were not visible (see Fig. 2.2). No information on the feedback conditions was provided, neither on their nature (except from visual feedback in substitution of force feedback) nor on the particular order with which they were going to be presented to the subject. Both the sequence of the feedback conditions and the initial position of the stiff constraint were randomized.

We carried out three experiments:

- *experiment #1*: twenty-four repetitions of the needle insertion task described above,
- *experiment #2*: two additional repetitions of the needle insertion task, during which the position of the stiff constraint was changed suddenly and unexpectedly,
- *experiment #3*: same as experiment #1, but in presence of a time delay in the haptic loop.

The first experiment aimed at demonstrating that (1) there is no relevant degradation of performance in the task when haptic feedback is substituted with cutaneous feedback, and that (2) using cutaneous-only feedback leads to better performances with respect to visual feedback in substitution of force feedback. Moreover, the experiment investigated if the localization of the cutaneous feedback on the fingertips responsible for handling the needle is an important factor.

The second experiment aimed at showing that using the cutaneous devices prevents the handle (and so the needle) from moving in unwanted directions in case of sudden and unpredictable changes of the position of the stiff constraint.

The third experiment aimed at confirming the well known result that there are no instability behaviors, not even in presence of delays, while using cutaneous feedback devices.

### ***2.3.3 Experiment #1: Comparison of the Feedback Conditions***

Sixteen participants (13 males, 3 females, age range 21–28) took part in the experiment, all of whom were right-handed. Eight of them had previous experience with haptic interfaces. None of the participants reported any deficiencies in the perception abilities. Each participant made 24 repetitions of the needle insertion task, with six randomized trials for each feedback condition:

- *visual feedback* by the moving horizontal bar (condition VF);
- *haptic feedback* by the grounded haptic interface (condition HF);

- *cutaneous feedback* by the ungrounded devices, provided to the hand holding the handle (condition CF);
- *cutaneous feedback* by the ungrounded devices, provided to the contralateral hand (condition CCF).

The experiment lasted 9.13 min on average, including the two additional repetitions of experiment #2, which followed the twelfth and the 24th repetitions of experiment #1 (see Sect. 2.3.4 for details). Subjects thus performed a total of 26 trials, whereof 24 were included in the results of experiment #1.

With the aim of comparing the different feedback conditions, we recorded the position  $x_n$  of the needle, steered by the subject's hand, and the penetration inside the stiff constraint  $p = \bar{x}_{sc} - x_n$ . The average penetration  $\bar{p}$  and the maximum penetration  $\bar{p}_M$  were analyzed. Data resulting from different trials of the same condition, performed by the same subject, were averaged before comparison with other conditions. Such values provide a measure of accuracy (average penetration) and overshoot (maximum penetration) in reaching the target depth. A null value in both metrics denotes the best performance, while a positive value indicates that the subject overran the target. Both measures can be considered particularly relevant to the surgical task, as an excessive penetration of the needle can result in permanent damage of tissues.

Figure 2.3 shows the positions of the needle (red patch) and of the tissue surface (green patch) versus time. The time of different trials was synchronized at the time the needle first enters the constraint ( $t = 0$ ), while positions were divided by the depth of the stiff constraint, which varied randomly among trials, and are presented as percentage. Trajectories were averaged among subjects for each feedback condition, and average trajectories plus/minus standard deviations are shown. The position of the stiff constraint (dashed red line, 100 %) and the initial position of tissue surface (dashed green line, 0 %) are shown as well. The black lines represent the instants when the average trajectory enters the tissue (left line) and when the sound beep is played (right line).

Figures 2.4 and 2.5 show, respectively, the average and maximum penetrations beyond the stiff constraint for each feedback condition (means and standard deviations are plotted). All column data passed the D'Agostino-Pearson omnibus K2 normality test. Comparison of the means among the feedback conditions was tested using one-way repeated measures analysis of variance (ANOVA). The means of average penetration (Fig. 2.4,  $F_{3,45} = 106.5$ ,  $p < 0.001$ ) and the means of maximum penetration (Fig. 2.5,  $F_{3,45} = 81.89$ ,  $p < 0.001$ ) differed significantly among the feedback conditions. Posthoc analyses (Bonferroni's multiple comparison test) revealed statistically significant difference between all pairs of conditions, both in terms of average penetration (Fig. 2.4,  $p < 0.001$  for all pairs) and in terms of maximum penetration of the needle (Fig. 2.5,  $p < 0.05$  for CF vs. CCF, and  $p < 0.001$  for all other pairs). Results indicate that the proposed sensory subtraction condition (CF) yields an intermediate performance between haptic feedback (HF, best performance) and visual feedback (VF, worst performance), in terms of both average and maximum penetration beyond the stiff constraint. These results demonstrate also

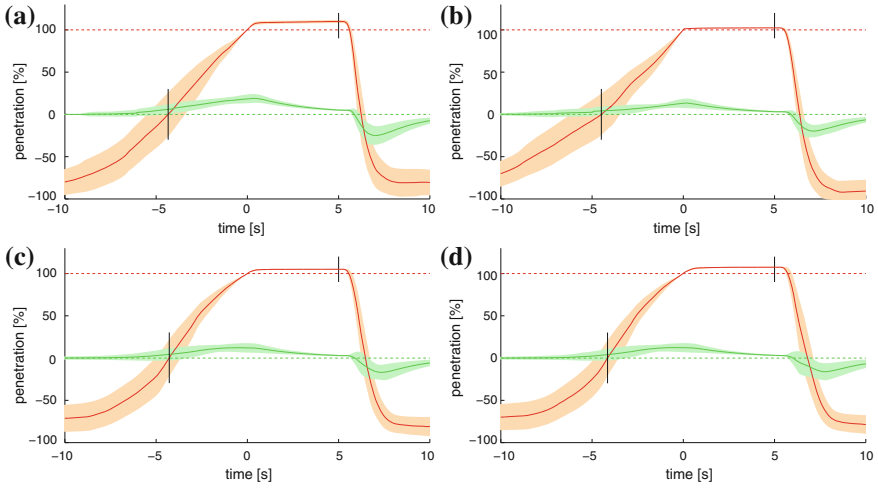


**Fig. 2.3** Penetration of the needle (*red patch*) and position of the tissue surface (*green patch*) versus time for experiment #1. Average trajectories among subjects and their standard deviations are plotted. The position of the stiff constraint (*dashed red line*) and the initial position of tissue surface (*dashed green line*) are shown as well. The *black lines* represent the instants when the average trajectory enters the tissue (*left line*) and when the sound beep is played (*right line*). **a** Visual feedback (VF). **b** Haptic feedback (HF). **c** Cutaneous feedback on the hand holding the handle (CF). **d** Cutaneous feedback on the contralateral hand (CCF) (color figure online)

**Fig. 2.4** Experiment #1: average penetration beyond the stiff constraint (mean and SD), for the visual (VF), haptic (HF) and cutaneous feedback modes (CF, CCF). A null value of this metric indicates high accuracy in reaching the target depth

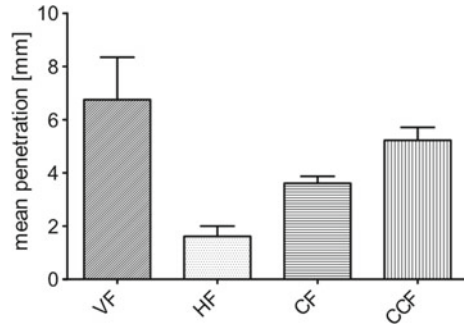


**Fig. 2.5** Experiment #1: maximum penetration beyond the stiff constraint (mean and SD), for the visual (VF), haptic (HF) and cutaneous feedback modes (CF, CCF). A null value of this metric indicates no overshoot in reaching the target depth

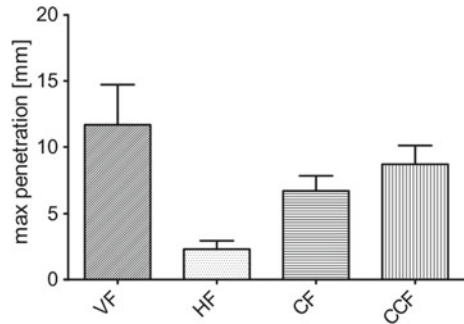
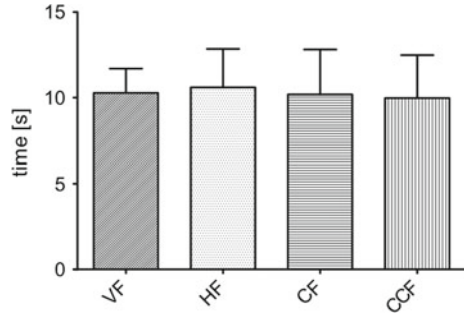




**Fig. 2.6** Experiment #1: time elapsed (mean and SD) between the first contact with the tissue and the sound played after 5 s of continuous contact with the stiff constraint, for the visual (VF), haptic (HF) and cutaneous feedback modes (CF, CCF)



that the cutaneous devices provide a more reliable form of feedback if applied to the fingertips which are responsible for holding the end-effector (CF) with respect to contralateral hand stimulation (CCF), suggesting that the localization of cutaneous feedback is crucial in this setting. Nonetheless, cutaneous feedback is more effective than visual feedback (VF) even when it is applied to the contralateral hand (CCF), indicating that not only the localization but also the nature of the sensation provided is relevant to the performance of the task.

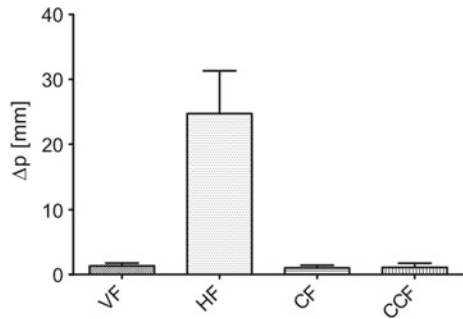
Figure 2.6 shows the average time elapsed between the instant the needle penetrates the tissue and the instant it reaches 5 s of continuous contact with the stiff constraint. Column data failed to pass the normality test, so we used the Friedman non-parametric test to analyze variance. Results indicate that there is no statistically significant difference between the feedback conditions in this metric. We may read this result by saying that the subjects became equally confident with all the feedback conditions proposed.

### 2.3.4 Experiment #2: Sudden Change of the Stiff Constraint

This second experiment evaluated the effect on needle position of a sudden and unpredictable change of the position of the stiff constraint, in the presence of the four feedback conditions described before (visual, haptic and the two cutaneous). The needle insertion task was the same as that described in Sect. 2.3.3. However, after 5 s of continuous contact, the depth of the stiff constraint was increased unexpectedly, so that the virtual environment suddenly fed back no force to the user. At the same time, the sound beep was produced as in the other repetitions of the needle insertion task, signaling the subject to extract the needle.

The test was performed during two additional repetitions of experiment #1. To ensure the surprise effect, each subject performed only two additional repetitions (using two different feedback conditions). A total of 32 trials were thus recorded for experiment #2: 8 trials for each feedback condition, performed by eight different subjects. The first additional trial was run after the 12th trial of experiment #1, the second after the 24th. No information was provided to the subjects about the

**Fig. 2.7** Experiment #2: difference (mean and SD) between the maximum penetration, after the movement of the stiff constraint, and the average penetration registered before (during continuous contact), for the visual (VF), haptic (HF) and cutaneous feedback modes (CF, CCF)



additional trials, which followed immediately the previous ones. A 30s rest was given to all subjects after the first additional trial, before continuing with the second part of experiment #1. Subjects did not know that the position of the stiff constraint was going to change and that they were performing a different task with respect to the others.

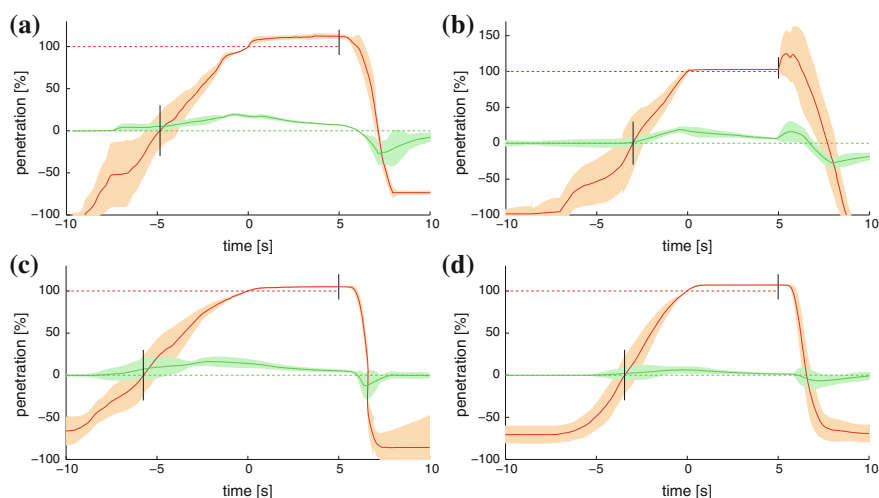
Figure 2.7 shows the difference  $\Delta p$  between the maximum penetration registered after the perturbation and the average penetration observed in the 5 s before (continuous contact). All column data passed the D'Agostino-Pearson omnibus K2 normality test. Comparison of the means among the feedback conditions was tested using one-way ANOVA (no repeated measures). The means differed significantly among the feedback conditions ( $F_{3,28} = 100.3$ ,  $p < 0.001$ ). Posthoc analyses (Bonferroni's multiple comparison test) revealed statistically significant difference between haptic feedback (HF) and each alternate condition (VF, CF, CCF,  $p < 0.001$ ). Results indicate that the presence of kinesthetic feedback may induce significantly greater unwanted motions of the needle with respect to the three non-kinesthetic feedback modes used in the experiments (the visual and the two cutaneous-only conditions). In fact, when the constraint moves during the haptic condition (HF), the subject's arm is counteracting an external force which suddenly drops.

Figure 2.8 shows the positions of the needle (red patch) and of the tissue surface (green patch) versus time for experiment #2. Data were synchronized, normalized and averaged among subjects as for the charts of Fig. 2.3.

### 2.3.5 Experiment #3: Stability with Time Delay

As other sensory substitution techniques, the main advantage of the proposed sensory subtraction approach is that it makes the haptic loop intrinsically stable. No instability behaviors occur, even in presence of large delays.

To support this hypothesis, we carried out a third experiment. We used the same protocol of experiment #1, including the feedback conditions and number of repetitions (24) per subject, but we introduced a delay of 50 ms in the haptic loop, between



**Fig. 2.8** Penetration of the needle (*red patch*) and position of the tissue surface (*green patch*) versus time for experiment #2, with the stiff constraint suddenly removed after 5 s of continuous contact. Average trajectories among subjects and their standard deviations are plotted. The position of the stiff constraint (*dashed red line*) and the initial position of tissue surface (*dashed green line*) are shown as well. The *black lines* represent the instants when the average trajectory enters the tissue (*left line*) and when the stiff constraint is removed and the sound beep is played (*right line*). **a** Visual feedback (VF). **b** Full haptic feedback (HF). **c** Cutaneous feedback on the hand holding the handle (CF). **d** Cutaneous feedback on the contralateral hand (CCF) (color figure online)

the virtual environment and either the haptic handle, the cutaneous devices or the visual rendering of force. Recent literature denotes the relevance of delays in teleoperated surgical tasks [10]. It is worth noting that instability of haptic feedback in the presence of time delays can be addressed by designing appropriate control systems [11–13]. Nonetheless, to emphasize the intrinsic stability of cutaneous feedback, this method was not used in the trials.

Ten participants (8 males, 2 females, age range 20–26) took part in the experiment, all of whom were right-handed and five of whom had previous experience with haptic interfaces. None of the participants reported any deficiencies in the perception abilities. The experiment lasted 8.39 min on average.

Figure 2.9 shows the positions of the needle (red patch) and of the tissue surface (green patch) versus time for experiment #3. A video of a representative run showing the instability issue is available as supplemental material at <http://extras.springer.com/978-3-319-25455-5> and at <http://goo.gl/Zf0QAB>. Data were synchronized, normalized and averaged among subjects as for Fig. 2.3. By comparing the charts with those in Fig. 2.3, we can notice that the instability occurred only with haptic feedback, i.e., only in the presence of the kinesthetic part of the interaction. Significant oscillations of the needle are likely to bring not only a greater penetration of the needle in the stiff constraint, but also a longer task completion time.

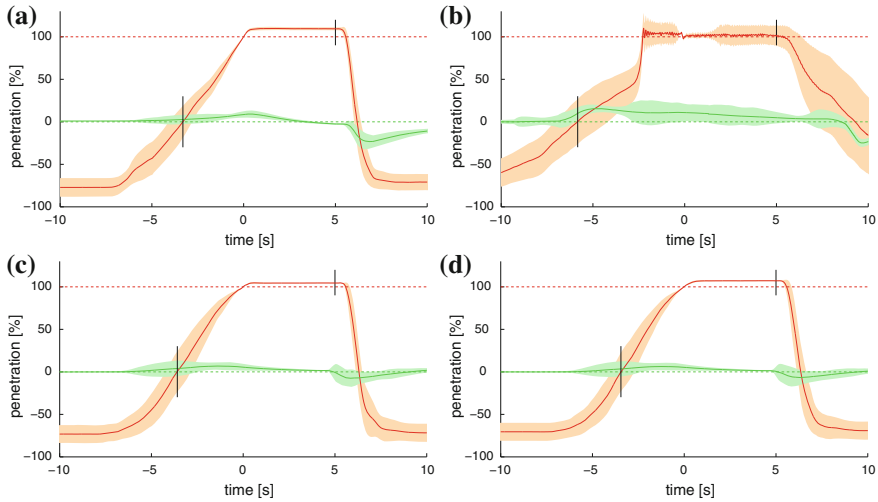


**Fig. 2.9** Penetration of the needle (*red patch*) and position of tissue surface (*green patch*) versus time for experiment #3, with a 50 ms network delay in the haptic loop. Average trajectories among subjects and their standard deviations are plotted. The position of the stiff constraint (*dashed red line*) and the initial position of tissue surface (*dashed green line*) are shown as well. The *black lines* represent the instants when the average trajectory enters the tissue (*left line*) and when the sound beep is played (*right line*). **a** Visual feedback (VF). **b** Full haptic feedback (HF). **c** Cutaneous feedback on the hand holding the handle (CF). **d** Cutaneous feedback on the contralateral hand (CCF) (color figure online)

**Fig. 2.10** Experiment #3: maximum penetration beyond the stiff constraint (mean and SD), for the the visual (VF), haptic (HF) and cutaneous feedback modes (CF, CCF), with a 50 ms network delay in the loop

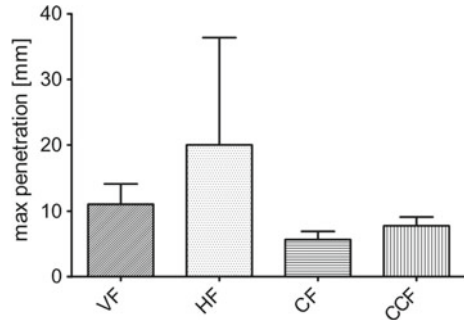
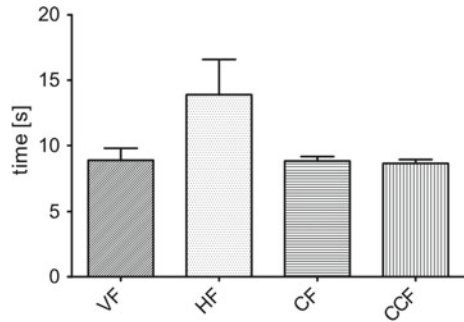


Figure 2.10 shows the maximum penetration beyond the constraint in the presence of the delay. Haptic feedback group data (HF) failed to pass the normality test, so the Friedman non-parametric test was used to analyze variance. The test indicated statistically significant difference between the feedback conditions ( $p < 0.001$ ). Posthoc analyses (Dunn's multiple comparison test) revealed statistically significant difference between haptic feedback (HF) and both cutaneous conditions (CF,  $p < 0.001$ ; CCF,  $p < 0.05$ ), and between cutaneous feedback (CF) and visual feedback (VF,  $p < 0.001$ ). Results indicate that the subjects, while receiving the

**Fig. 2.11** Experiment #3: time elapsed between the first contact with the tissue and the sound beep, for the visual (VF), haptic (HF) and cutaneous feedback modes (CF, CCF), with a 50 ms network delay in the haptic loop



full haptic feedback in the presence of a time delay, reached a significantly greater peak penetration in the stiff constraint with respect to that obtained while receiving feedback from the ungrounded cutaneous devices, regardless of the localization of cutaneous feedback. The same result was obtained when subjects received visual feedback of force instead of cutaneous feedback on the fingers which are responsible for handling the needle.

Figure 2.11 shows, for each feedback condition and in the presence of the time delay, the mean time elapsed between the first penetration in the tissue and the instant the needle reaches 5 s of stable contact with the stiff constraint. Haptic feedback and cutaneous feedback group data failed to pass the normality test, so the Friedman non-parametric test was used to analyze variance. The test indicated statistically significant difference between the feedback conditions ( $p < 0.001$ ). Posthoc analyses (Dunn's multiple comparison test) revealed statistically significant difference between haptic feedback (HF) and all other feedback conditions (VF,  $p < 0.01$ ; CF,  $p < 0.05$ ; CCF,  $p < 0.001$ ). Results indicate that the time needed to complete the task was significantly greater while receiving the kinesthetic feedback with respect to the other non-kinesthetic feedback conditions. Such a difference had not been observed in the absence of time delays (see Fig. 2.6), and must be related to instability.

## 2.4 Discussion

The first experiment evaluated the effectiveness of the sensory subtraction technique. The results of this experiment indicate that the subjects, while receiving visual feedback (VF) in substitution of force feedback, reached a significantly greater average and maximum penetration in the stiff constraint (worst performance) in comparison with that obtained while receiving either full haptic (HF) or cutaneous-only feedback (CF and CCF). Conditions CF and CCF provided intermediate performance between visual and haptic feedback. No difference between groups was observed in terms of task completion time.

As expected, full haptic feedback outperformed all the other feedback conditions. The cutaneous-only condition proved itself to be more intuitive than the other sensory substitution technique, regardless of the localization of the cutaneous devices (either on the hand performing the task or on the contralateral hand). However, when the cutaneous force feedback was applied to the contralateral hand (i.e., the one not controlling the grounded interface), performance degraded with respect to the case when the cutaneous force feedback was applied to the active hand. A possible interpretation could be that the cutaneous feedback applied to the contralateral hand needs time for transcallosal transmission to reach the hemisphere controlling the operating hand. In fact, the feedback reaches the hemisphere of the brain not involved in the motor control of the hand moving the input device, and for this reason may require more time to be transformed in motor action [14].

These results suggest that the sensory subtraction approach can be successfully used in substitution of traditional haptic feedback, with a significant improvement of performance with respect to visual sensory substitution techniques. Not only the type of feedback, cutaneous rather than visual, but also the place where it is applied is important. The best performance is in fact obtained when the cutaneous devices are worn on the hand involved in the task. This result can be explained by considering that the area of application of the force and the particular design of the cutaneous devices proposed provide the user with a direct and intuitive measure of the contact force being substituted, thus producing a more natural interaction with the device.

However, during the first experiment, performance degraded when kinesthetic feedback information was removed (HF vs. CF). One possible explanation is that kinesthetic force played a role in arm dynamics during the execution of the needle insertion task. In particular, the virtual force helped the subject in stopping hand motion when the stiff constraint was reached, which is the main reason for using stiff constraints indeed. Conversely, in the proposed cutaneous-only condition, no physical aid is provided to the user to accomplish the task, so any arm motion derives entirely from motor control. The resulting benefit is that unwanted motions can be drastically reduced in critical situations, as shown in experiment #2. Nonetheless, without adequate sense of touch, achieving normal and top performance in tasks that require high levels of dexterity is extremely difficult [15]. Moreover, even simple tactile information can be effective, both in virtual and in real environments. For example, major gains in body posture control in real environments can be obtained from minimal touch information applied to a fingertip [16]. This may explain why cutaneous only tasks were better executed than the substituted visual condition tasks (VF).

One major advantage of sensory subtraction is that, despite the fact that the interaction is closer to haptic rendering, no unwanted movements are likely to be produced during the execution of guided tasks. This achievement, that is corroborated by the results of experiment #2, is crucial in applications where safety is paramount, such as robot-aided surgery, in which unwanted movements of the surgeon's hand induced by knesthetic feedback may produce serious damages to the patient. The absence of unwanted movements, even in the case of sudden and unpredictable changes of the position of the stiff constraint, can be explained by considering that, in the cutaneous

feedback conditions, kinesthetic feedback is completely missing, so that subjects can maintain a stable contact with the stiff constraint without exerting an active force on the handle.

The last experiment showed that, in the presence of a transmission delay, full haptic feedback can bring the system near to instability, as significant oscillations of needle position occurred, whereas cutaneous (and visual) feedback allows a stable contact with the stiff constraint surface. The occurrence of instability with a relatively small time delay may be due to the particular (stiff) setting of the experimental device used in the experiments. However, the fact that kinesthesia can bring instability in haptic teleoperation in the presence of time delays is well-known in the literature of haptics and teleoperation.

Another drawback of using full haptic feedback in presence of transmission delays is the longer time needed to complete the task. Statistical analysis on task completion times showed that, in case of no delay, there are no significant differences between the four different feedback conditions, while in the presence of a network delay, task completion time using haptic feedback can be significantly greater than that obtained using cutaneous-only feedback.

## 2.5 Conclusions

The work presented in this chapter showed how cutaneous feedback applied to the thumb and index finger pads can be effectively used to substitute full haptic feedback in robotic teleoperation. The main advantage of using cutaneous feedback is that the stability of the haptic loop is intrinsically guaranteed. This can be very convenient for critical applications such as robotic surgery. Chapter 4 will address and analyze the use of cutaneous feedback in robotic surgery systems. Note also that actuation for cutaneous displays usually requires less power and it is less bulky than that required to provide haptic feedback, with a direct effect on simplifying mechanical design and reducing costs.

The main drawback of the proposed approach is that, like for other sensory substitution techniques, the performance is lower than that of full haptic feedback. However, differently from other substitution techniques, our approach conveys force feedback exactly where it is expected and provides the subject with a direct and co-located perception of the contact force. This degradation of performance with respect to full haptic feedback approaches is the main motivation that pushed us toward solutions mixing cutaneous and kinesthetic stimuli, as I will further discuss in Chap. 5. Another weak point of the work presented in this chapter is that the experiments were carried out in a simulated 1-DoF scenario. In the next chapters we will extend our evaluation of the sensory subtraction approach to more challenging scenarios. Chapter 3 considers a remote peg-in-hole task, both in simulated and real environments. Chapter 4 presents an application of the sensory subtraction idea in a remote palpation task using the da Vinci Surgical System.

## References

1. D. Prattichizzo, C. Pacchierotti, G. Rosati, Cutaneous force feedback as a sensory subtraction technique in haptics. *IEEE Trans. Haptics* **5**(4), 289–300 (2012)
2. J.J. Abbott, P. Marayong, A.M. Okamura, Haptic virtual fixtures for robot-assisted manipulation. *Robot. Res.* 49–64 (2007)
3. D. De Lorenzo, E. De Momi, I. Dyagilev, R. Manganelli, A. Formaglio, D. Prattichizzo, M. Shoham, G. Ferrigno, Force feedback in a piezoelectric linear actuator for neurosurgery. *Int. J. Med. Robot. Comput. Assist. Surg.* **7**(3), 268–275 (2011)
4. B. Davies, Robotic devices in surgery. *Minim. Invasive Ther. Allied Technol.* **12**(1), 5–13 (2003)
5. K. Minamizawa, S. Fukamachi, H. Kajimoto, N. Kawakami, S. Tachi, Gravity grabber: wearable haptic display to present virtual mass sensation, in *Proceeding of the ACM Special Interest Group on Computer Graphics and Interactive Techniques Conference* (2007), p. 8–es
6. B. Dasgupta, T.S. Mruthyunjaya, The stewart platform manipulator: a review. *Mech. Mach. Theory* **35**(1), 15–40 (2000)
7. D. Prattichizzo, F. Chinello, C. Pacchierotti, M. Malvezzi, Towards wearability in fingertip haptics: a 3-dof wearable device for cutaneous force feedback. *IEEE Trans. Haptics* **6**(4), 506–516 (2013)
8. S. Cotin, H. Delingette, N. Ayache, Real-time elastic deformations of soft tissues for surgery simulation. *IEEE Trans. Vis. Comput. Gr.* **5**(1), 62–73 (1999)
9. C.B. Zilles, J.K. Salisbury, A constraint-based god-object method for haptic display, in *Proceedings IEEE/RSJ International Conference on Intelligent Robots and Systems*, vol. 3 (1995), pp. 146–151
10. I. Nisky, A. Pressman, C.M. Pugh, F.A. Mussa-Ivaldi, A. Karniel, Perception and action in teleoperated needle insertion. *IEEE Trans. Haptics* **4**(3), 155–166 (2011)
11. G. Niemeyer, J.J.E. Slotine, Stable adaptive teleoperation. *IEEE J. Ocean. Eng.* **16**(1), 152–162 (1991)
12. Y. Ye, P.X. Liu, Improving haptic feedback fidelity in wave-variable-based teleoperation orientated to telemedical applications. *IEEE Trans. Instrum. Measurement* **58**(8), 2847–2855 (2009)
13. T.M. Lam, M. Mulder, M.M. Van Paassen, Haptic feedback in UAV tele-operation with time delay. *J. Guidance, Control Dyn.* **31**(6), 1728–1739 (2008)
14. E.R. Kandel, J.H. Schwartz, T.M. Jessell et al., *Principles of Neural Science* (McGraw-Hill, New York, 2000)
15. G. Robles-De-La-Torre, The importance of the sense of touch in virtual and real environments. *IEEE Multimed.* **13**(3), 24 (2006)
16. J.J. Jeka, P. Ribeiro, K. Oie, J.R. Lackner, The structure of somatosensory information for human postural control. *Mot. Control* **2**(1), 13–33 (1998)



Cutaneous Haptic Feedback in Robotic Teleoperation

Pacchierotti, C.

2015, XXII, 142 p., Hardcover

ISBN: 978-3-319-25455-5